

White organic light-emitting devices with CdSe/ZnS quantum dots as a red emitter

Yanqin Li, Aurora Rizzo, Marco Mazzeo, Luigi Carbone, Liberato Manna, Roberto Cingolani, and Giuseppe Gigli^{a)}

National Nanotechnology Laboratory (NNL) of Istituto Nazionale di Fisica della Materia (INFN), Lecce University, Via Arnesano Km 5, Lecce I-73100, Italy

(Received 16 February 2005; accepted 4 April 2005; published online 23 May 2005)

White hybrid organic/inorganic light-emitting devices (LEDs) have been fabricated by using stable red-emitting CdSe/ZnS core-shell quantum dots (QDs) covered with a trioctylphosphine oxide organic ligand. The device-active structure consists in a host/guest system with a blue-emitting poly[(9,9-dihexyloxyfluoren-2,7-diyl)-alt-co-(2-methoxy-5-{2-ethylhexyloxy}phenylen-1,4-diyl)] (PFH-MEH) polymer doped with red-emitting QDs and a green emitting metal chelate complex Alq₃, with improved electron injection and transfer properties. A fairly pure white OLED with Commission Internationale de l'Eclairage coordinates of (0.30,0.33) is fabricated by accurate control of the Förster energy and charge-transfer mechanisms between the different device constituents obtained by tuning the concentration ratio of the QDs/PFH-MEH blend. In particular, charge-transfer processes to CdSe/ZnS core-shell quantum dots are found to be the key element for well-balanced white emission. Maximum external quantum efficiency up to 0.24% at 1 mA cm⁻² and 11 V in air atmosphere are reported, showing that hybrid LEDs can be a promising route towards more stable and efficient light-emitting devices for lighting applications. © 2005 American Institute of Physics. [DOI: 10.1063/1.1921341]

I. INTRODUCTION

White organic light-emitting devices (OLEDs) have attracted much interest for their potential applications in flat, large area displays,¹ and recently in the lighting industry. So far, a number of white OLEDs have been fabricated.²⁻⁷ To obtain white light, all the three primary colors (red, green, and blue) have to be produced simultaneously. Since it is difficult to obtain all primary emissions from a single molecule, excitation of more than one organic species is often necessary, thus introducing color stability problems. Due to the different degradation rate of the employed organic compounds, the emission color of the device can, in fact, change with time. Recently, several groups have reported the use of II-VI semiconductor nanocrystals, such as CdSe, in combination with polymers, in the fabrication of LEDs.⁸⁻¹¹ The CdSe semiconductor quantum dots (QDs) exhibit a size-dependent color variation due to quantum confinement effects, which covers almost the whole visible range.¹² Additionally, the fluorescence efficiency and, in particular, the stability of the nanocrystals can be greatly improved by modifying the particle surface. These characteristics can be merged with peculiar properties of organic materials, such as flexibility and ease of processing, to give rise to a novel class of low-cost hybrid white-emitting devices with improved lifetime and color stability.¹³⁻¹⁶ However, despite the promise of these systems, so far, fewer studies have been reported on hybrid white light-emitting devices based on QDs and the emission mechanisms not yet deeply investigated. Host-guest systems are typically employed to obtain white light emis-

sion by exploiting two mechanisms, namely, Förster energy transfer¹⁷⁻¹⁹ and charge transfer.^{20,21} In the Förster mechanism, dipole-dipole coupling results in a nonradiative transfer of the singlet excited-state energy from a donor molecule to an acceptor molecule. In the charge-transfer mechanism, an excited guest molecule is formed by the sequential transfer of separate hole and electron charges to the guest molecule from different host molecules in the surrounding matrix. All these processes have to be accurately controlled in order to obtain white electroluminescence.

Here, we report a hybrid white light-emitting device based on a blend of poly[(9,9-dihexyloxyfluoren-2,7-diyl)-alt-co-(2-methoxy-5-{2-ethylhexyloxy}phenylen-1,4-diyl)] (PFH-MEH) and CdSe/ZnS QDs and a layer of Alq₃ that combines the ease of processibility of polymer materials, good electron transfer and injection properties, and efficient luminescence of metal chelate complexes (Alq₃) with the narrow-band emission and color stability of QDs. A fairly pure white OLED with Commission Internationale de l'Eclairage (CIE) (0.30,0.33) and electroluminescence (EL) efficiency of 0.24%, to our knowledge the best value so far reported for hybrid white light-emitting diodes based on QDs, is realized via incomplete energy and charge transfer by tuning the concentration ratio of the QDs/PFH-MEH blend. Both the emission mechanisms have been investigated by carrying out photoluminescence and electroluminescence measurements on active structures with different QDs/PFH-MEH ratio. We demonstrated that a balanced white emission is obtained in hybrid ternary systems PFH-MEH:QDs/Alq₃ when Förster energy transfer in the guest-host system is accomplished by charge transfer from PFH-MEH and Alq₃ to QDs during the electrical excitation.

^{a)}Author to whom correspondence should be addressed; electronic mail: gigli@mailing.unile.it

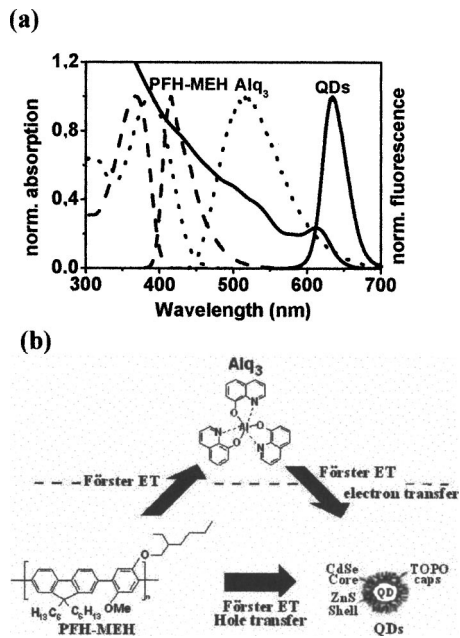


FIG. 1. (a) Absorption (left) and photoluminescence (right) spectra for PFH-MEH (dash), Alq₃ (dot), and QDs (solid); (b) chemical structures of components and possible energy-transfer charge-transfer pathways.

II. EXPERIMENT

A. Synthesis of CdSe/ZnS core/shell QDs

The CdSe/ZnS QDs were prepared according to standard procedure.^{22,23}

B. Fabrication of hybrid electroluminescence devices

The chemical structures of the active materials used in the devices and a schematic diagram of the device structure are shown in Figs. 1(b) and 3(a), respectively. Devices consisting of ITO//PEDOT-PSS//PFH-MEH:CdSe/ZnS//Alq₃//Ca/Al were fabricated as follows. A hole-transporting layer (100 nm) of poly(3,4-ethylenedioxythiophene):poly(styrenesulfonate) (PEDOT-PSS), used to lower the hole-injection barrier at the indium tin oxide (ITO) surface, was spin-deposited onto the cleaned ITO-coated glass substrate (120 nm, 15 Ω). The layer was then heated at 110 °C for 10 min. Then, a layer of a 5-nm-sized CdSe/ZnS QDs and PFH-MEH polymer blend (100 nm) was spin coated from a chloroform solution on the surface of the PEDOT-PSS. QDs concentration was calculated using the Lambert-Beer law: $A = \epsilon LC$, where A is the absorption peak for a given sample, C is the molar concentration (mol/l) of the nanocrystals, L is fixed at 1 cm, and ϵ is the extinction coefficient (5.94×10^5 l/mol cm is measured at first exciton peak; the diameter is 5.11 nm).²⁴ Finally, 10-nm-thick layer Alq₃, acting as electron-injecting/electron-transferring and electron-emitting material, and a 50-nm-thick Ca cathode covered with a 150-nm-thick Al layer were deposited by thermal evaporation at a pressure of 4×10^{-6} mbars. Three devices with a different concentration ratio of the PFH-MEH/QDs blend constituents and a reference one without the Alq₃ layer were fabricated.

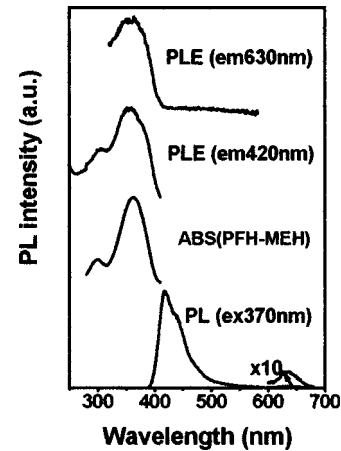


FIG. 2. PL and PLE spectra of the film for device ITO//PEDOT-PSS//PFH-MEH:CdSe/ZnS//Alq₃//Ca/Al with the ratio of PFH-MEH:CdSe/ZnS = 100:1 and absorption spectrum of PFH-MEH film.

C. Characterization

Photoluminescence (PL) and excitation photoluminescence (PLE) measurements were performed on thin films and CHCl₃ solutions by using a Cary Eclipse fluorescence spectrophotometer with an intense xenon flash lamp. Absorption (abs) measurements were carried out using a Cary 5000 UV-Vis spectrophotometer. The electroluminescence (EL) spectra were measured by an Ocean optics CCD (S2000) spectrometer. Voltage-luminance-current characteristics were measured by using a Keithley source measurement unit (Keithley 2700 and Keithley 2400) with an amplified silicon photodiode (RS 303-674, Hamamatsu). All the measurements were performed at room temperature in air atmosphere.

III. RESULTS AND DISCUSSION

Host-guest systems are typically employed to obtain white light, i.e., a higher-energy-emitting host material (donor) is doped with lower-energy-emitting guest materials (acceptor) to promote energy transfer from the host to the guest. The rate of this energy transfer and Förster radius²⁵ are given in the following expressions:

$$k_{\text{Förster}} = \tau_d^{-1} (R_0/r)^6,$$

$$R_0^6 = \alpha \int_0^\infty F_d(\nu) \epsilon_a(\nu) \nu^{-4} d\nu,$$

where τ_d is the lifetime of the donor in the absence of the acceptor, r is the distance between the donor and acceptor, R_0 is the Förster radius, and $F_d(\nu)$ and $\epsilon_a(\nu)$ are the fluorescence and extinction spectra of the donor and acceptor, respectively. According to this expression, the necessary condition for Förster transfer occurrence is not a negligible overlap of the acceptor absorption and donor photoluminescence spectra and a maximum distance between the two constituents of 30–50 Å. Both these conditions are verified for the host/guest system PFH-MEH/CdSe:ZnS QDs, in which the two components are closely intermixed in the blend and show substantial abs and PL spectra overlap [see Fig. 1(a)]. A clear spectral overlap between the PFH-MEH emission and the

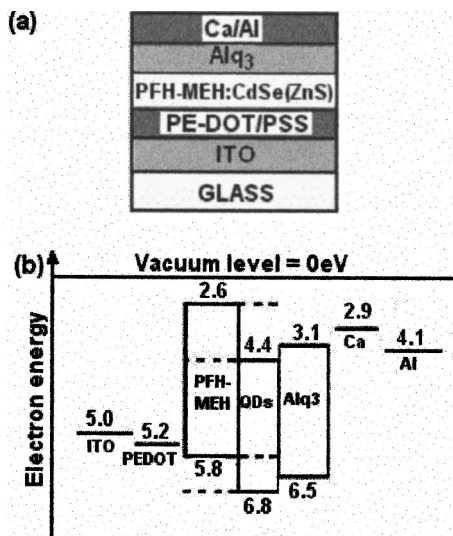


FIG. 3. (a) The device configuration, (b) proposed energy-level diagram of the device ITO//PEDOT-PSS//PFH-MEH:CdSe/ZnS//Alq₃/Ca/Al.

QDs absorption and between the Alq₃ PL and QDs abs is also observed. The possible Förster energy-transfer pathways between different components are indicated in Fig. 1(b). In order to obtain white emission, all these processes have to be accurately controlled and, in particular, incomplete energy transfer from the host PFH-MEH to CdSe/ZnS QDs has to be induced. To this aim a detailed characterization of the emission mechanisms has been performed by the photoluminescence (PL) and photoluminescence excitation (PLE) measurements on bilayers of PFH-MEH:CdSe/ZnS//Alq₃ with a relative concentration of PFH-MEH/QDs of 100:1 (Fig. 2). Two emission bands at 635 and 420 nm are observed while exciting at 370 nm, which originate from the CdSe/ZnS QDs and PFH-MEH, respectively. Negligible emission is instead observed from Alq₃. The weakness of the QDs and Alq₃ band evidences the excessive PFH-MEH concentration and a limited energy transfer to the two low-energy-emitting species. PLE spectra with detection wavelengths fixed at 420 and 630 nm, corresponding to the emission peaks of PFH-MEH and CdSe/ZnS QDs, respectively, overlap the absorption of PFH-MEH, showing that the emission of CdSe/ZnS QDs originates mainly from the excitation energy transferred from PFH-MEH.

Electroluminescence measurements have been carried out on ITO//PEDOT-PSS//PFH-MEH:CdSe/ZnS//Alq₃/Ca/Al structures [see Fig. 3(a)]. In Fig. 4 the EL spectra for different PFH-MEH:CdSe/ZnS concentration ratios are reported. Contrary to the PL spectrum when a 100:1 ratio is used, a strong quenching of the PFH-MEH emission and an increase of the Alq₃ and QDs bands is observed. This suggests the occurrence of novel and more efficient transfer

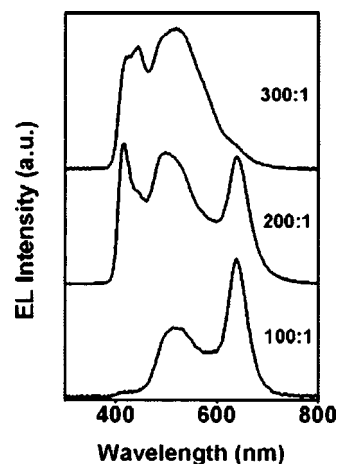


FIG. 4. Electroluminescence spectra for the device ITO//PEDOT-PSS//PFH-MEH:CdSe/ZnS//Alq₃/Ca/Al with different ratio (PFH-MEH:CdSe/ZnS, c%).

mechanisms from the blue-emitting polymer and green-emitter Alq₃ to the lower-energy-emitting species QDs. In particular, in the case of electrically driven devices, in addition to the Förster energy transfer, several charge-transfer pathways can occur. Possible pathways leading to emissive states are shown in Fig. 5.

The physical basis for a charge transfer was studied extensively by Marcus,²⁶ and a first-order model of the rate of transfer between the donor and acceptor molecule is given in

$$k_{ct} = \nu_0 \exp[-\beta(r - r_0)] \exp(\Delta G^*/kT),$$

where ν_0 is a collision frequency, r is the distance from the donor to the acceptor, β and r_0 are measures of the electronic coupling between the donor and acceptor, and ΔG^* is the free-energy barrier. Since the hopping mechanism requires overlap of the molecular orbitals of the donor and host molecules, charge transfer is typically limited to a maximum distance of 5–10 Å. Such distances exist between blended PFH-MEH and QDs and at the interface Alq₃/PFH-MEH:QDs. However, in core-shell QDs the ligands which bind to the nanocrystal surface act as barriers to electron charge transfer in the semiconductor core. Thus, we expect an efficient electron charge injection in QDs only at the interface with the Alq₃, which is characterized by much higher electron transporting and injecting properties.

In order to achieve white EL emission, the different color components have to be accurately balance by controlling both the Förster energy-transfer and charge-transfer mechanisms. To this aim we fabricated devices with different PFH-MEH:QDs concentration ratios, namely, 200:1 and 300:1. At low QDs concentration (300:1), the possible pathway are processes I and II. Process I involves the transfer of

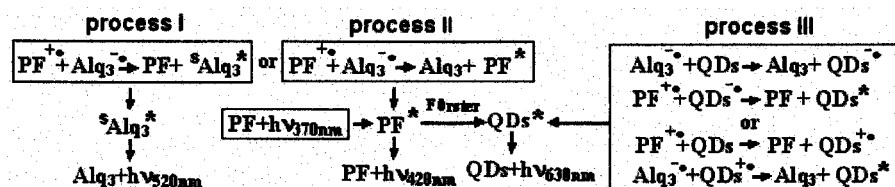


FIG. 5. Possible pathways leading to emissive states in device ITO//PEDOT-PSS//PFH-MEH (PF):CdSe/ZnS//Alq₃/Ca/Al. Radical cation, radical anion, and singlet excited-state molecules are indicated by (•)⁺, (•)⁻ and (•)⁰, respectively.

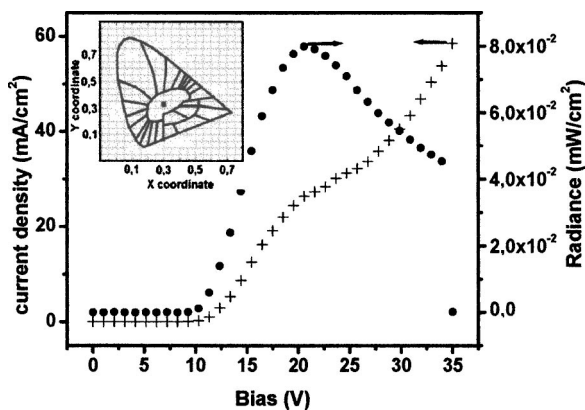


FIG. 6. V - I , V - L characteristics of device ITO//PEDOT-PSS//PFH-MEH:CdSe(200:1)/ZnS//Alq₃//Ca/Al. Inset: CIE coordinates (0.30,0.33) are indicated.

a hole from a PFH-MEH cation radical (PF⁺) to a Alq₃ anion radical (Alq₃⁻). Process II involves the transfer of an electron from a Alq₃ anion radical (Alq₃⁻) to a PFH-MEH cation radical (PF⁺). Both the mechanisms result in excited Alq₃ and PFH-MEH molecules which can decay radiatively, originating blue and green EL emission. Negligible red emission instead originated from the amount of QDs. By increasing the concentration of CdSe/ZnS QDs (concentration ratio 200:1), the possible pathways are processes I, II, and III. A relevant additional role is assured by the following processes: Förster energy transfer to QDs from excited PFH-MEH and Alq₃ molecules sequential charge transfer of a hole from PFH-MEH followed by the transfer of an electron from Alq₃ or charge transfer of an electron from Alq₃ followed by the transfer of a hole charge from PFH-MEH (process III in Fig. 5). An efficient emission at the three primary colors is thus obtained from PFH-MEH, Alq₃, and QDs with a balanced white spectrum with CIE (0.30,0.33). In Fig. 6 voltage-current (V - I) and voltage-luminance (V - L) characteristics of the device ITO//PEDOT-PSS//PFH-MEH:CdSe/ZnS(200:1)//Alq₃//Ca/Al are reported. Maximum luminance of 8×10^{-2} mW/cm² at 20 V and a turn-on voltage of 9 V are measured in air atmosphere. Maximum external quantum efficiency of 0.24% is measured at 1 mA cm⁻² and 11 V, to our knowledge the best results so far reported for hybrid white OLEDs based on QDs. Such improved values can be explained by considering the device energy-level diagram in Fig. 3(b). Work functions, band gaps, and electron affinities of ITO, Ca, Al, PEDOT-PSS, PFH-MEH, CdSe/ZnS QDs, and Alq₃ are taken from literature.^{8,9,11} In these QD-based LEDs, holes are considered to be injected from the ITO electrode through the PEDOT:PSS layer into the polymer hole conductor and are eventually transported to the QDs. Similarly, the electrons are considered to be injected from the Ca/Al cathode into the Alq₃ and are eventually transported to the QDs. Since the high electron affinity of QDs the electrons are better confined

within the surface of PFH-MEH:QDs/Alq₃, thus enhancing the balance between opposite carriers in the region where a more efficient radiative exciton recombination can occur.

IV. CONCLUSIONS

Hybrid organic/inorganic light-emitting devices (LEDs) have been fabricated by using stable red-emitting CdSe/ZnS core-shell quantum dots blended in a blue emitting PFH-MEH polymer. A thin layer of an electron-injecting and electron-transporting metal chelate complex Alq₃ is used to accurately control and balance the Förster energy-transfer and charge-transfer processes between the different active components, allowing a fairly pure white OLED with CIE (0.30,0.33) and EL efficiency of 0.24%. These results are a first step towards a novel class of hybrid devices for lighting applications combining the stability properties of colloidal inorganic nanocrystals with the flexibility and ease of fabrication of organic LED technology.

- ¹J. R. Sheat, H. Antoniadis, M. Hueshen, W. Leonard, J. Miller, R. Moon, D. Roitman, and A. Stocking, *Science* **273**, 884 (1996).
- ²X. H. Zhang, M. W. Liu, O. Y. Wong, C. S. Lee, H. L. Kwong, S. T. Lee, and S. K. Wu, *Chem. Phys. Lett.* **369**, 478 (2003).
- ³K. O. Cheon, and J. Shinar, *Appl. Phys. Lett.* **81**, 1738 (2002).
- ⁴Y. S. Huang, J. H. Jou, W. K. Weng, and J. M. Liu, *Appl. Phys. Lett.* **80**, 2782 (2002).
- ⁵R. S. Deshpande, J. Brooks, V. Bulovic, and S. R. Forrest, *Adv. Mater. (Weinheim, Ger.)* **14**, 147 (2002).
- ⁶J. Thompson, R. I. R. Blyth, M. Mazzeo, M. Anni, G. Gigli, and R. Cingolani, *Appl. Phys. Lett.* **79**, 560 (2001).
- ⁷G. Cheng, Y. Zhao, Y. F. Zhang, and S. Y. Liu, *Appl. Phys. Lett.* **84**, 4457 (2004).
- ⁸J. L. Zhao, J. Y. Zhang, C. Y. Jiang, J. Bohnenberger, T. Basche, and A. Mews, *J. Appl. Phys.* **96**, 3206 (2004).
- ⁹H. Yang and P. H. Holloway, *J. Phys. Chem. B* **107**, 9705 (2003).
- ¹⁰M. C. Schlamp, X. G. Peng, and A. P. Alivisatos, *J. Appl. Phys.* **82**, 5837 (1997).
- ¹¹S. Coe, W. K. Woo, M. Bawendi, and V. Bulovic, *Nature (London)* **420**, 800 (2002).
- ¹²A. P. Alivisatos, *J. Phys. Chem.* **100**, 13226 (1996).
- ¹³V. L. Colvin, M. C. Schlamp, and A. P. Alivisatos, *Nature (London)* **370**, 354 (1994).
- ¹⁴M. C. Schlamp, X. Peng, and A. P. Alivisatos, *J. Appl. Phys.* **82**, 5837 (1997).
- ¹⁵M. Gao, C. Lesser, S. Kirstein, H. Mohwald, A. L. Rogach, and H. Weller, *J. Appl. Phys.* **87**, 2297 (2000).
- ¹⁶B. O. Dabbousi, M. G. Bawendi, O. Onitsuka, and M. F. Rubner, *Appl. Phys. Lett.* **66**, 1316 (1995).
- ¹⁷T. Förster, *Discuss. Faraday Soc.* **7**, 27 (1959).
- ¹⁸N. J. Turro, *Modern Molecular Photochemistry* (Benjamin/Cummings, Menlo Park, CA, 1978).
- ¹⁹J. R. Lakowicz, *Principles of Fluorescence Spectroscopy* (Plenum, New York, 1983).
- ²⁰K. Utsugi and S. Takanok, *J. Electrochem. Soc.* **139**, 3610 (1992).
- ²¹H. Suzuki and S. Hoshino, *J. Appl. Phys.* **79**, 8816 (1996).
- ²²P. Reiss, J. Bleuse, and A. Pron, *Nano Lett.* **2**, 781 (2002).
- ²³T. Pellegrino *et al.*, *Nano Lett.* **4**, 703 (2004).
- ²⁴W. W. Yu, L. H. Qu, W. Z. Guo, and X. G. Peng, *Chem. Mater.* **15**, 2854 (2003).
- ²⁵S. E. Shaheen, B. Kippelen, and N. Peyghambarian, *J. Appl. Phys.* **85**, 7939 (1999).
- ²⁶R. A. Marcus and N. Sutin, *Biochim. Biophys. Acta* **811**, 265 (1985).